AIP | Review of Scientific Instruments

Low noise current-to-voltage converter and vibration damping system for a low-temperature ultrahigh vacuum scanning tunneling microscope

Laurent Libioulle, Alexandra Radenovic, Eva Bystrenova, and Giovanni Dietler

Citation: Review of Scientific Instruments **74**, 1016 (2003); doi: 10.1063/1.1533100
View online: http://dx.doi.org/10.1063/1.1533100
View Table of Contents: http://scitation.aip.org/content/aip/journal/rsi/74/2?ver=pdfcov
Published by the AIP Publishing

Low noise current-to-voltage converter and vibration damping system for a low-temperature ultrahigh vacuum scanning tunneling microscope

Laurent Libioulle,[a] Alexandra Radenovic, Eva Bystrenova, and Giovanni Dietler
Institut de Physique de la Matière Condensée, Université de Lausanne, CH-1015 Lausanne, Switzerland

(Received 24 April 2002; accepted 24 October 2002)

The design of low-temperature tunnel current converters and the design of a low-temperature damping stage for a scanning tunneling microscope (STM) are presented. The current amplifiers are able to measure very low tunnel current (down to 0.25 pA), while preserving a sufficient bandwidth for topographic and spectroscopic measurements and with very low noise characteristics (down to 3 fA $Hz^{-1/2}$). The design of a compact low-temperature magnetic damping stage with a resonance frequency of about 7 Hz, protecting the microscope mechanics against mechanical vibrations of the cryostat is also described. The damped stage with the microscope mechanics is in contact with the cryostat during cooling, while during the STM measurements, it is mechanically isolated. © *2003 American Institute of Physics.* [DOI: 10.1063/1.1533100]

I. INTRODUCTION

In order to improve the stability of the tunnel junction and of the atoms or molecules imaged by the tip, many low-temperature ultrahigh vacuum (UHV) scanning tunneling microscopes (STMs) were developed.[1–12] For high-quality STM measurements, one has to be able to measure small currents, while reaching low-level tunnel current noise and a sufficient bandwidth. Therefore, the development of efficient current–voltage ($I-V$) converters is required. Very often, for operation at low temperature, external amplifiers are connected to the tunnel junction through at least 1 m of copper wire.[2] This connection picks up electromagnetic and mechanical noise due to temperature fluctuations and cryostat vibrations, but the most limiting factor is the drastic increase of the capacitance of the line. Therefore, reaching a bandwidth of few hundred Hz for tunnel currents in the range of pA is a challenge. Few cryoamplifiers have been successfully designed[13–15] but most of the time at the cost of less flexibility for changing from one tunnel current range to another. Special electronic components have to be selected with great care in order to dissipate heat as low as possible,[16] and to work properly especially in the case of liquid-helium temperature.[17,18]

In this article, we will describe the design of external room-temperature preamplifiers managing tunnel current ranging from 0.25 pA to 50 nA, having a sufficient bandwidth for topographic and spectroscopic measurements, and presenting very low noise characteristics. Afterward, we will present a way to further reduce the thermal noise of the feedback resistor of the converter, by placing only this resistor in contact with the cryostat,[19] close to the microscope while keeping sufficient bandwidth. By this simple way, we transform the room-temperature amplifier to a so-called ''low-temperature'' amplifier. Concerning the vibration damping, cryostats and shielding system render the design of the STM damping stage very complicated.[20] Because of operating at low temperature, Viton-type materials have to be avoided for damping stages and the use of long springs can make the design delicate.[21]

Most of the cryogenic systems use one or two external pneumatic suspension stages to filter the mechanical vibrations but they are not efficient in eliminating the vibrations produced inside the cryostat itself. The situation is complicated by the acoustic noise, which is picked up by the surface of the whole UHV system and transmitted to the STM mechanics through the bellows and tubes. We will describe the way to reduce the mechanical noise by designing a compact low-temperature magnetic damping stage, which protects the tunnel junction from the vibrations of the cryostat produced by the boiling of the cryogenic liquid inside the tank.

II. ROOM-TEMPERATURE PREAMPLIFIER DESIGN

The tunnel current flowing from the biased tip toward the sample has to be amplified and converted to a voltage. This is done through a measuring resistor across which a voltage drop takes place. The resistor could also be a feedback resistor of an extremely low bias current operational amplifier. Measuring pA current leads to the use of resistors ranging at least from 1 to 10 GΩ. However, the major problem turns out to be the shunt capacitance associated with the feedback resistor. This capacitance is in the range of 1 pF and will limit the bandwidth of the preamplifier to about 150 Hz in the case of 1 GΩ feedback resistor. The limited bandwidth of the $I-V$ converter will reduce the maximum scanning speed and lower the modulation frequency for spectroscopic measurements (or worse, it will increase the amplitude needed for the modulating signal). In both cases, the scanning time is increased, making an STM image more sensitive to thermal drift and mechanical vibrations. An easy method to increase the bandwidth, while keeping the noise level as low as possible, consists in the introduction of an RC feedback network[13,22] in order to exactly compensate the

[a]Electronic mail: laurent.libioulle@ipmc.unil.ch

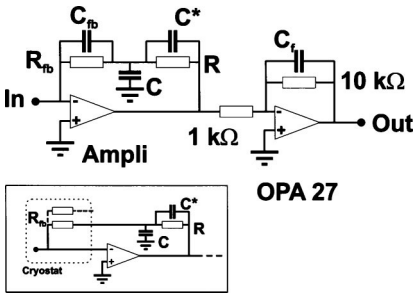

FIG. 1. Electronic diagram of the room-temperature $I-V$ converter. The RC feedback network is introduced in the feedback loop to compensate the shunt capacitance of the large value feedback resistor R_{fb}. The converter is a two-stage amplifier. The gain of the second stage is always fixed to 10, whereas the gain of the first stage ranges from 10^7 to 10^{10}. For the first amplifier type, see Table I. In the case of the low-temperature converter, the feedback resistor R_{fb} is fixed to the cryostat as indicated in the inset.

shunt capacitance of the feedback resistor. We have designed our $I-V$ converters as a two-stage amplifier. In Fig. 1, the basic configuration of such an amplifier is presented. Four different amplifiers have been prepared, each of them specially designed for one range of tunnel current and covering at least 2 orders of magnitudes of current variation. In Table I, the values of the needed components are given as well as the measured noise as a stand-alone device. For the RC compensating network, we have used a 1 MΩ resistor to negligibly modify the value of the feedback resistor (less than 1%). In the case of ideal compensation, the RC product in the compensating network has to be equal to the product of the feedback resistor and its shunt capacitance. Toward this end, first C value is estimated from the converter bandwidth without any compensation and, subsequently, is experimentally adjusted to insure a large bandwidth. Then, C^* is inserted and its value adjusted in order to cut the highest-frequency noise resulting from the perfect compensation of the shunt capacitance.

Figure 2 presents a typical 200 Å×200 Å unfiltered STM image of a silver surface Ag(111). The sample temperature was maintained at 50 K (solid nitrogen) and the iridium tip[23] was biased with 3 mV. The Z scale of the image is 0.5 Å from black to white and no bias modulation technique was used to improve the contrast. We can clearly distinguish the scattering by impurities and defects of the electronic density of state corresponding to the surface state electrons confined in the two-dimensional plane. On the same surface the spectrum of the preamplifier output was measured with the feedback loop open. The spectrum is shown in Fig. 3 with the tip in tunnel condition (curve 1) and retracted (curve 2). The 25 fA $\mathrm{Hz}^{-1/2}$ base line measured as a stand-alone amplifier (Table I) fit the spectrum nicely in the case of retracted position, indicating that the entire UHV system is not adding noise to the converter. In tunnel conditions, the clear deviation from the base line indicates that tip stability, thermal drift, mechanical vibrations, and acoustic noise all contribute to the tunnel current noise. The largest components range from 0 to about 50 Hz and are probably mostly generated by mechanical vibrations of the nitrogen tank. It becomes clear from the comparison of the converter output spectra, that the mechanical stability of the tunnel junction should be improved in order to reach more stable conditions. This clearly indicates that the addition of a low-temperature damping stage is one key element to improve the tunnel junction stability. We will describe this point later. However, one can also reduce the base line noise level. This noise is generated

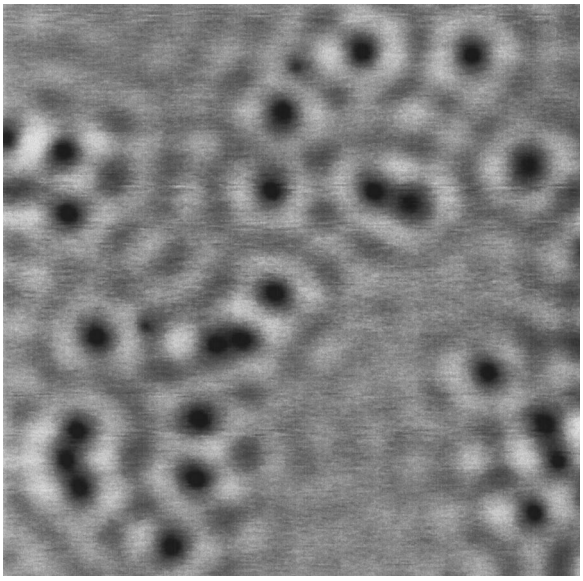

FIG. 2. STM image of a 200 Å×200 Å Ag(111) surface. The Z scale of the image is 0.5 Å, from black to white. The tip is made out of iridium wire. The tunnel measuring conditions were 3 mV bias voltage, 100 pA tunnel current, and 10^9 converter gain with feedback resistor at room temperature. The surface state electrons of the Ag(111) are confined in the direction perpendicular to the surface plane. The surface state electrons form a clearly visible standing wave pattern around defects and impurities.

TABLE I. Values and characteristics of each electronic component used to build the tunnel current converters. The gain ranges from 10^8 to 10^{11}. The bandwidth was measured by applying a sinusoidal signal with a 10^8 Ω resistor to the input, while the peak-to-peak noise was determined from the oscilloscope trace. The rms current noise over the bandwidth is calculated from these values.

Gain	Amplifier	R_{fb}	C_{fb} (pF)	R	C	C^* (pF)	C_f (nF)	Bandwidth (Hz)	Noise (mV ptop)	Noise rms (fA $\mathrm{Hz}^{-1/2}$)
$T=300$ K										
10^8	OPA111	10 MΩ	5.6	⋯	⋯	⋯	6.2	2.5 K	<1	71
10^9	OPA111	100 MΩ	2.7	1 MΩ	82 pF	220	6.2	1.3 K	2.5	25
10^{10}	OPA128	1 GΩ	⋯	1 MΩ	680 pF	330	68	500	6	9.5
10^{11}	OPA128	10 GΩ	⋯	1 MΩ	2 nF	100	150	370	15	2.8
$T=50$ K										
10^{10}	OPA128	1 GΩ	⋯	1 MΩ	6.8 nF	220	68	~350	~1.5	3

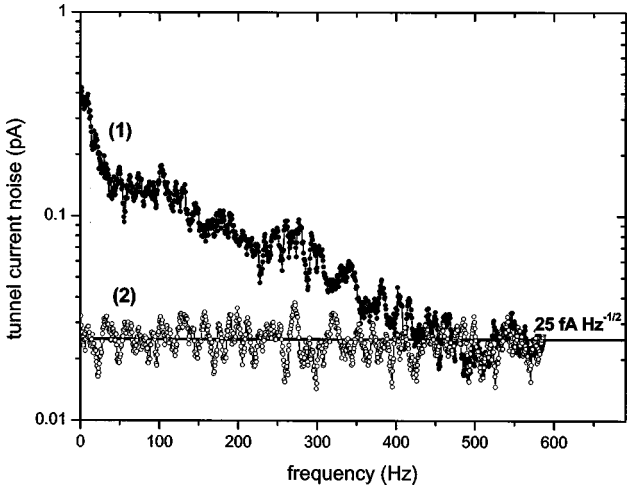

FIG. 3. Noise spectrum of the 10^9 gain converter under tunnel conditions (Ir tip, 3 mV bias, and 100 pA tunnel current) on a Ag(111) sample surface (curve 1) and in retracted position (curve 2). The 25 fA $Hz^{-1/2}$ base line nicely fit the noise spectrum of the retracted tip, whereas in tunnel conditions there is a clear deviation from white noise attributed to acoustic noise and mechanical vibrations of the nitrogen tank on which the cryostat is screwed.

by the measuring resistor inside the $I-V$ converter and is due to *shot noise* and *Johnson noise*.[24,25] The *shot noise*, related to the discrete nature of the current, makes the current of independent charges fluctuate around the mean value I_{dc} over a frequency interval Δf as given by

$$I_{\text{shot}}=(2eI_{\text{dc}}\Delta f)^{1/2}. \tag{1}$$

On the other hand, the *Johnson noise* results from the thermal motion of electrons through the feedback resistor. This noise depends directly on the temperature T and for a resistor R is given over a frequency interval Δf by

$$I_{\text{Johnson}}=(4k_BT\Delta f/R)^{1/2}. \tag{2}$$

Reducing the temperature of the resistor will directly lower the *Johnson noise* of the feedback resistor (without affecting the *shot noise*) and, subsequently, will reduce the measured noise at the output of the preamplifiers.

III. LOW-TEMPERATURE PREAMPLIFIER DESIGN

The main idea for designing low-temperature converters is simply to remove the feedback resistor from the room-temperature converter box and to place it in contact with the STM cryostat. The reason for doing this is that the feedback resistor is the main source of noise, which can be easily eliminated. The resistor is placed inside the UHV chamber, in thermal contact with the cryostat and as close as possible to the microscope. The resistor,[26] which is encapsulated within a ceramic tube is glued on a sapphire plate. This sapphire plate provides very good thermal contact with the wall of the cryostat and excellent electrical isolation. The feedback resistor, placed at low temperature, is thus electrically connected to the converter electronics working at room temperature. Only one additional UHV electrical feedthrough is needed to operate the converter in the low-temperature mode. The original connection from the tunnel junction remains unchanged. One side of the low-temperature feedback resistor is permanently connected to the tunnel junction, as close as possible to the STM body, whereas the other side of this resistor is connected to the additional electrical feedthrough (see inset of Fig. 1). In order to operate at different gains, several low-temperature feedback resistors can be permanently connected to the tunnel junction and each of them needs to have its own isolated electrical output. The change from one gain to another is made by selecting the corresponding output feedthrough. We point out also that this configuration allows one to continue to use a normal room-temperature converter, since the original tunnel current feedthrough is unchanged, and to switch to a low-temperature configuration only when the noise has to be reduced to an extremely low level. In our microscope, one low-temperature resistor (1 GΩ) was permanently connected. In the case of normal measurements, no additional noise coming from the unused low-temperature feedback resistors has been detected if the unused electrical feedthrough is simply shielded by a BNC cap to avoid pick-up electromagnetic noise. Compared to the usual room-temperature converter, the addition of new electrical wires (from the tunnel junction to the low-temperature resistor and from that resistor to a new electrical feedthrough) results in an increase of the total shunt capacitance. We have estimated that the resulting capacitance is in the order of 10 pF for low-temperature connections. However, the adjustment of the value in the RC feedback network makes it easy to compensate this increase of the shunt capacitance, allowing us to maintain the bandwidth for low-temperature converters. The new values of the RC network needed for keeping the bandwidth of the 10^{10} low-temperature converter are indicated in Table I in the case of 1 GΩ inside feedback resistor. It is more difficult to measure the bandwidth at a low temperature than for a standalone preamplifier, but we evaluate the bandwidth to be larger than 350 Hz for a 10^{10} gain.

In Table II, we calculate the theoretical *Johnson noise* and the *shot noise* for a tunnel current ranging from 1 pA to

TABLE II. Calculation of the theoretical *Johnson noise* and *shot noise* for the nominal current of each converter. The Johnson noise is evaluated at room-temperature (300 K) and at solid nitrogen temperature (50 K). The total rms noise corresponds to the theoretical limit of our two-stage converters.

Gain	Current (pA)	Output (mV)	Johnson noise (300 K) (fA $Hz^{-1/2}$)	Johnson noise (50 K) (fA $Hz^{-1/2}$)	Shot noise (fA $Hz^{-1/2}$)	Total noise rms (300 K) (fA $Hz^{-1/2}$)	Total noise rms (50 K) (fA $Hz^{-1/2}$)
10^8	10^3	100	41	17	18	45	25
10^9	10^2	100	12.8	5.2	5.7	14	7.7
10^{10}	10	100	4.1	1.7	1.8	4.5	2.5
10^{11}	1	100	1.3	0.5	0.57	1.4	0.8

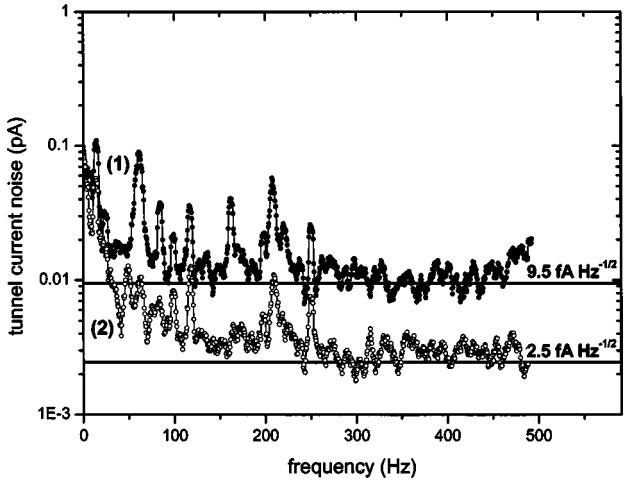

FIG. 4. Experimental comparison between room-temperature (curve 1) and low-temperature (curve 2) noise spectrum in the case of the 10^{10} gain converters in exactly the same tunnel conditions (same Ir tip, 3 mV bias, and 10 pA; same position on the Ag(100) sample). The 9.5 fA $Hz^{-1/2}$ noise base line of the room-temperature converter corresponds to the measured value for the stand-alone converter reported in Table I and fits the noise spectrum at high frequency (curve 1), while at low frequency there are clear peaks appearing. These peaks are attributed to acoustic and mechanical vibrations of the nitrogen tank. The 2.5 fA $Hz^{-1/2}$ base line for curve 2 corresponds to the minimum noise limit level for our low-temperature 10^{10} gain converter as reported in Table II, calculated from theoretical values. The experimental noise spectrum is better fit with a 3 fA $Hz^{-1/2}$ base line, corresponding to about 1.5 mV peak-to-peak fluctuation signal at the output of the converter as indicated in Table I.

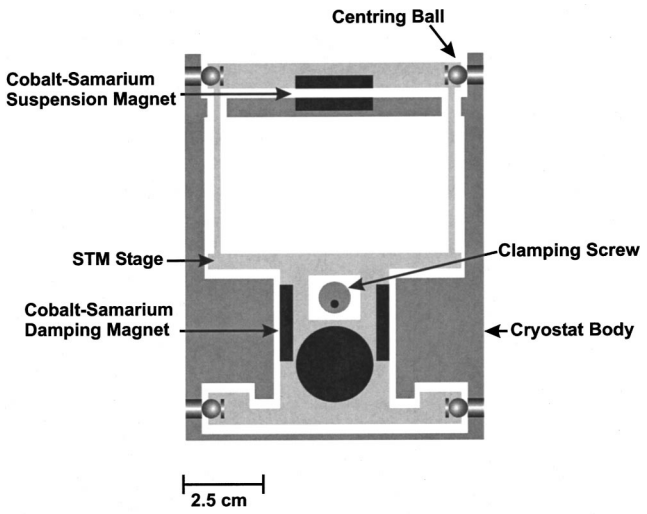

FIG. 5. Overview of the low-temperature magnetic damping stage. The STM stage is suspended by magnetic repulsion between two cobalt–samarium magnets and damped by four cobalt–samarium magnets through an eddy-current damping mechanism. The STM stage is centered inside the cryostat body by six balls, which are held in place magnetically and which are freely rolling on graphite rods and plates attached to the fixed and to the mobile parts, respectively. The STM stage is completely shielded by the cryostat body and could also be pushed in contact by turning the clamping screw during cooling periods.

1 nA and the resulting root-mean-square (rms) noise is given in the case of room-temperature and low-temperature (50 K) converters. The theoretical noise level limit for a two-stage 10^{10} converter, as we have used so far, is 2.5 fA $Hz^{-1/2}$ at 50 K.

The comparison between the experimental noise spectrum of a 10^{10} room-temperature converter (curve 1) and the spectrum of the equivalent low-temperature converter (curve 2) is shown in Fig. 4. The noise level has been lowered from 9.5 to about 3 fA $Hz^{-1/2}$ which is close to the theoretical limit of 2.5 fA $Hz^{-1/2}$. At a low frequency (roughly below 50 Hz), we see clearly that the noise level of the low-temperature preamplifier is rising up from the base level toward the room-temperature noise spectrum. As we have already seen in Fig. 3, this confirms that the origins of this noise are mechanical vibrations and instabilities. However, imaging silver surfaces by STM using the cryoconverter has demonstrated that the image quality was improved because of this noise reduction. This improvement was estimated to be equivalent to a *Z*-signal noise reduction of about 0.1 Å in the case of scanning an Ag(100) flat surface. On the other hand, the scanning speed, time constant, and gain of the STM feedback loop remain the same, confirming that the bandwidth of the cryoamplifier was maintained large enough for standard imaging and spectroscopic measurements.

IV. LOW-TEMPERATURE DAMPING STAGE DESIGN

The room-temperature STM's are generally isolated from mechanical vibrations by springs and Viton damping stages. Viton material is efficient against acoustic coupling, while the spring stage or pendulum system protects the microscope against very low-frequency vibrations. As was already mentioned, at low temperature, the stiffness of such springs increases rapidly, making the damper less efficient, while Viton stages have to be completely ruled out. The most simple solution turns out to be the use of one or two external pneumatic suspension stages for damping the external mechanical vibrations and to design the microscope to be as rigid as possible. But this could not be enough, since the flow of cryogenic liquid and the bubbles appearing inside the dewar remain a major source of noise. In order to improve the tunnel current stability, it is thus highly recommended to mechanically isolate the STM head from the cooling stage. Spring damping stages, especially designed for working at low temperature, have already been described[2,19] and special spring material needs to be used. The corresponding resonance frequency for such systems ranges from 2 to 10 Hz. One can also notice that increasing the length of metallic springs is one way to keep the resonance frequency of the damper as low as possible, but it will make the cryostat less compact. An other crucial point is the fact that through the spring wire, medium- and high-frequency vibrations could propagate and reach the microscope. It would be desirable to have, at a low temperature, a damping stage with the characteristics of a room-temperature Viton stage, which filters frequencies up to few kHz. However, we would like to keep the STM stage as small as possible, as stable as possible for tip and sample exchanges and, at the same time, decoupled from mechanical vibrations of the cryostat while keeping the low working temperature. In order to meet all of these goals, we have designed a low-temperature magnetic damping stage as shown in Fig. 5.

The copper STM stage, inside the copper body of the

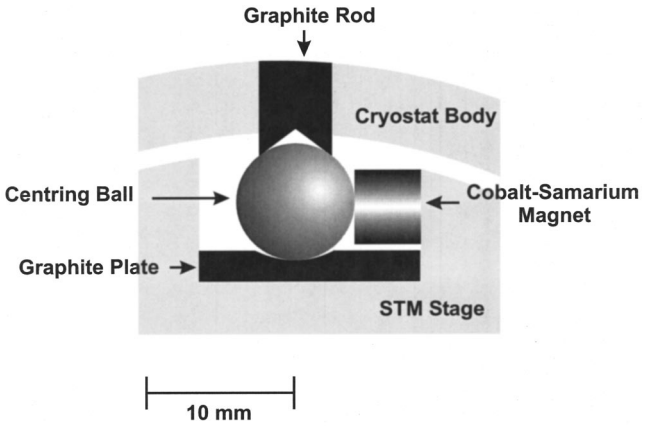

FIG. 6. Top view of the centering system using one 8 mm bearing ball, one 4 mm cobalt–samarium magnet, and two graphite pieces on which the ball is rolling freely. The contact surface is minimized and only two (one on the top and one on the bottom) over the six centering devices have a V-shaped graphite rod, the others being perfectly flat.

cryostat, is suspended by magnetic repulsion between two strong cobalt–samarium magnets, the first one is glued on the mobile stage and the second one; on the cryostat. The mobile stage is centered inside the cryostat by six 8 mm balls rolling on graphite surfaces and four large cobalt–samarium magnets attached to the mobile stage under the microscope provide eddy-current damping.[2] The copper body of the cryostat is tightly screwed to the cryogenic tank in order to provide excellent thermal contact.

In order to transmit as low vibration as possible from the tank to the STM through the cryostat body, as well as acoustic noise from the UHV chamber, the six centering balls have to move freely at a low temperature. Toward this end, each ball is just held in position by a cobalt–samarium magnet, as drawn in Fig. 6, but stays totally free to rotate around the axis perpendicular to the holding magnet. The ball can thus

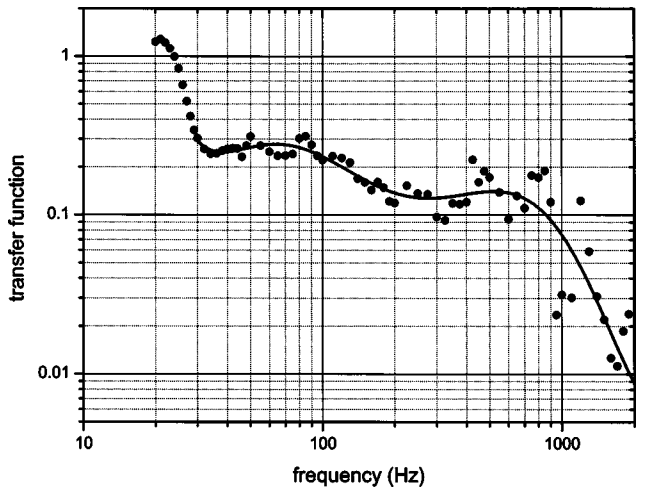

FIG. 7. Experimental transfer function of the low-temperature magnetic damping stage measured with an accelerometer from 20 Hz up to 2 kHz. The transfer function is defined as the ratio of the amplitude of vibrations detected on the STM stage and on the cryostat body. The resonance frequency of the damper is measured to be about 7 Hz. The cutoff takes place for a frequency higher than 20 Hz and attenuation by a factor of 4 is already reached for frequencies higher than 30 Hz. These filtering characteristics are similar to commonly used room-temperature Viton stacks.

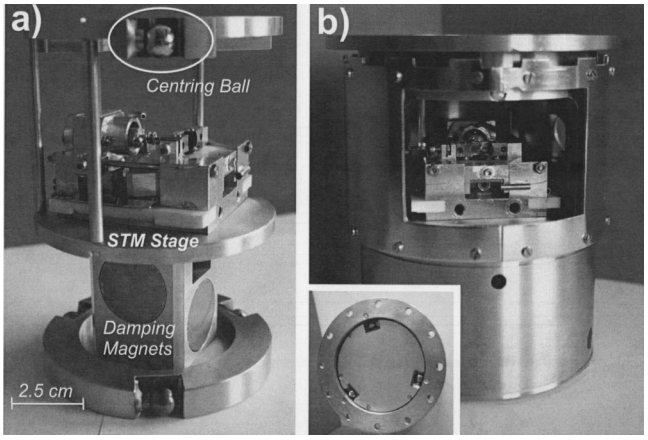

FIG. 8. Picture of the STM stage (a) and of the complete damping system (b). The magnetic damping cryostat described here is directly screwed at the bottom of the cryogenic tank.

turn and roll on the two graphite surfaces. Three centering balls on the top of the STM stage and three on the bottom are enough to keep the STM stage perfectly aligned inside the cryostat. During cooling, the STM stage is pushed into contact with the bottom plate of the cryostat by a clamping screw and will be released during the measurements. The mobile stage will stay in thermal equilibrium with the surrounding walls of the nonmovable parts. The resonance frequency of the system has been measured to be around 7 Hz by manually exciting the damping stage and detecting the oscillations with a coil in front of a magnet. The oscillations are completely damped in three to four periods. To characterize the efficiency of our magnetic damping stage, we have measured, with an accelerometer, its complete transfer function for frequencies higher than 20 Hz.

The experimental transfer function is shown in Fig. 7 and has been obtained by vibrating the damping setup while measuring the amplitude of the vibration on itself and on the STM stage using two accelerometer heads. The ratio between the two vibration amplitudes was calculated.[27] We clearly see that the magnetic damping stage acts as a low-pass filter and is efficient exactly like a room-temperature Viton stack. Lateral vibrations are probably less efficiently attenuated but the STM stage is only in contact with the cryogenic stage though six free-moving balls which are unable to transmit any stress to the STM stage. The picture of the STM stage is presented in Fig. 8(a). The eddy-current damping magnets are clearly visible below the microscope as well as the centering balls. The complete damping system is shown in Fig. 8(b).

The improvement of the mechanical design of our low-temperature STM, as well as the improvement of tunnel current converters, will allow us to image the morphology of epitaxial thin metal oxide layers in more stable conditions, where very low current, high spatial resolution, and spectroscopic measurements are needed to study the oxide barrier.[28]

ACKNOWLEDGMENTS

The authors would like to thank Dr. Santos Alvarado for continuous and stimulating discussions, Professor Wolf-

Dieter Schneider for providing instrumental facilities, and Samuel Allenspach, Rodolphe Gonzalez, Jean-René Moser, and Jacques Rittener for technical support. This work was supported by the Swiss National Science Foundation under Grants 2000-065160.01.

[1] R. Gaisch, J. K. Gimzewski, B. Reihl, R. R. Schlittler, M. Tchudy, and W. D. Schneider, Ultramicroscopy **42**, 1621 (1992).
[2] B. C. Stipe, M. A. Rezaei, and W. Ho, Rev. Sci. Instrum. **70**, 137 (1999).
[3] D. M. Eigler and E. K. Schweizer, Nature (London) **344**, 524 (1990).
[4] A. D. Kent, C. Renner, P. Niedermann, J. G. Bosch, and O. Fischer, Ultramicroscopy **42**, 1632 (1992).
[5] L. E. Harrell and P. N. First, Rev. Sci. Instrum. **70**, 125 (1999).
[6] E. T. Foley, A. F. Kam, and J. W. Lyding, Rev. Sci. Instrum. **71**, 3428 (2000).
[7] S. H. Pan, E. W. Hudson, and J. C. Davis, Rev. Sci. Instrum. **70**, 1459 (1999).
[8] L. Petersen, M. Schunack, B. Schaefer, T. R. Linderoth, P. B. Rasmussen, P. T. Sprunger, E. Laegsgaard, I. Stensgaard, and F. Besenbacher, Rev. Sci. Instrum. **72**, 1438 (2001).
[9] H. Zhang, U. Memmert, R. Houbertz, and U. Hartmann, Rev. Sci. Instrum. **72**, 2613 (2001).
[10] Y. Kondo, E. T. Foley, T. Amakusa, N. Shibata, S. Chiba, M. Iwatsuki, and H. Tokumoto, Rev. Sci. Instrum. **72**, 2977 (2001).
[11] T. H. Chang, C. H. Yang, M. J. Yang, and J. B. Dottellis, Rev. Sci. Instrum. **72**, 2989 (2001).
[12] H. Okamoto and D. Chen, Rev. Sci. Instrum. **72**, 4398 (2001).
[13] B. Michel, L. Novotny, and U. Dürig, Ultramicroscopy **42**, 1647 (1992).
[14] H. Birk, K. Osstveen, and C. Schnöneneberger, Rev. Sci. Instrum. **67**, 2977 (1996).
[15] S. Urazhdin, S. H. Tessmer, and R. C. Ashoori, Rev. Sci. Instrum. **73**, 310 (2002).
[16] A. T. Lee, Rev. Sci. Instrum. **64**, 2373 (1993).
[17] J. Imai and R. Flores, Rev. Sci. Instrum. **64**, 3024 (1993).
[18] A. T. Lee, Rev. Sci. Instrum. **60**, 3315 (1989).
[19] N. Moussy, H. Courtois, and B. Pannetier, Rev. Sci. Instrum. **72**, 128 (2001).
[20] E. W. Hudson, R. W. Simmonds, C. A. Y. Leon, S. H. Pan, and J. C. Davis, Czech. J. Phys. **46**, 2737 (1996).
[21] H. Jodicke, thesis No. 1986, Lausanne EPFL, 1999.
[22] C. J. Chen, *Introduction to Scanning Tunneling Microscopy* (Oxford University Press, New York, 1993).
[23] L. Libioulle, Y. Houbion, and J. M. Gilles, Rev. Sci. Instrum. **66**, 97 (1995); L. Libioulle, Y. Houbion, and J. M. Gilles, J. Vac. Sci. Technol. B **13**, 1325 (1995).
[24] P. Horowitz and W. Hill, *The Art of Electronics* (Cambridge University Press, Cambridge, UK, 1989).
[25] B. K. Jones, *Electronics for Experimentation and Research* (Prentice–Hall, London, 1986).
[26] Eltec Insttuments Inc., Daytona Beach, FL.
[27] M. Taborelli, L. Libioulle, M. Renier, and J. M. Gilles, Phys. Mag. **11**, 41 (1989).
[28] S. Schintke, S. Messerli, M. Pivetta, F. Patthey, L. Libioulle, M. Stengel, A. De Vita, and W. D. Schneider, Phys. Rev. Lett. **87**, 276801 (2001).